REFERENCES

[1] A. N. Didenko and S. A. Novikov, "Investigation of some high-frequency characteristics of elliptical waveguides with diaphragms," *Radio Eng. Electron. Phys.*, vol. 21, pp. 117–120, 1976.

[2] S. Washisu and I. Fukai, "Microwave heating of a dielectric slab by elliptical waveguides," *Trans. IECEJ*, vol. J 61-B, pp. 640–645, July 1978.

[3] G. I. Veselov, "Two-layer waveguide of elliptical cross-section," *Telecommun. Radio Eng.*, pt. 2, vol. 22, pp. 100–105, 1967.

[4] A. I. Kovshov and V. Ya. Smorgonskiy, "Critical conditions in an elliptical waveguide with a dielectric rod," *Radio Eng. Electron. Phys.*, vol. 13, pp. 630–633, 1968.

[5] V. Ya. Smorgonskiy, "Computation of critical frequencies in a partially filled elliptical waveguide," *Radio Eng. Electron. Phys.*, vol. 16, pp. 1812–1817, 1971.

[6] V. Ya. Smorgonskiy, "Analysis of dispersion equation of a two-layer elliptical waveguide in critical regime," *Radio Eng. Electron. Phys.*, vol. 17, pp. 1011–1013, 1972.

[7] A. A. Radionov and V. Ya. Smorgonskiy, "Waveband properties of a two-layer elliptical waveguide," *Radio Eng. Electron. Phys.*, vol. 18, pp. 129–132, 1973.

[8] S. B. Rayevskiy, L. G. Simkina, and V. Ya. Smorgonskiy, "Distribution of electromagnetic field of the HE_{11} mode in the transverse cross-section of a double layer elliptical waveguide," *Radio Eng. Electron. Phys.*, vol. 18, pp. 985–990, 1973.

[9] Yu. Ilarionov and V. Ya. Smorgonskiy, "Dispersion equation of the HE_{11} mode in a double layer elliptical waveguide for $v_p = c$," *Radio Eng. Electron. Phys.*, vol. 21, pp. 124–126, 1976.

[10] V. Ya. Smorgonskiy, Yu. A. Ilarionov, and V. F. Barinova, "A second-order approximation of the dispersion equation for the HE_{11} mode in an elliptical waveguide containing a dielectric rod," *Radio Engin. Electron. Phys.*, vol. 21, pp. 16–20, 1976.

[11] Yu. A. Ilarionov and V. Ya. Smorgonskiy, "Investigation of dispersion equations of an elliptical waveguide with an insert for $v_p = c$," *Radio Eng. Electron. Phys.*, vol. 23, pp. 14–17, 1978.

[12] S. R. Rengarajan and J. E. Lewis, "The elliptical surface wave transmission line," this issue, pp. 000–000.

[13] C. Yeh, "Elliptical dielectric waveguides," *J. Appl. Phys.*, vol. 33, pp. 3235–3243, 1962.

[14] J. G. Kretzschmar, "Wave propagation in hollow conducting elliptical waveguides," *IEEE Trans. Microwave Theory Tech.*, vol. MTT-18, pp. 547–554, Sept. 1970.

[15] ——, "Attenuation characteristics of hollow conducting elliptical waveguides," *IEEE Trans. Microwave Theory Tech.*, vol. MTT-20, pp. 280–284, Apr. 1972.

The Elliptical Surface Wave Transmission Line

SEMBIAM R. RENGARAJAN, MEMBER, IEEE AND J. E. LEWIS, SENIOR MEMBER, IEEE

***Abstract*—Electromagnetic wave propagation on an elliptical cross-sectional surface-wave transmission line is investigated theoretically. Characteristic equations for odd and even hybrid modes are derived and solved numerically. Expressions are obtained for power flow, energy storage and power loss using a perturbation method. Numerical results on propagation characteristics of three lower order modes are presented. The $_eHE_{11}$ mode is shown to have low attenuation particularly at high eccentricities. The propagation characteristics of lines of high eccentricities are found to be slowly varying functions of dimensions.**

I. INTRODUCTION

SINGLE WIRE transmission lines and dielectric coated conductors of circular cross sections have been studied extensively [1]–[5]. King and Wiltse [4] have shown that the circular Goubau line has application in millimeter wave propagation because of low attenuation. Cutoff wave numbers of several low-order modes in Goubau lines have been reported recently [5]. The even dominant mode in elliptical dielectric rod and tube waveguides has been shown to have lower attenuation than the corresponding mode in circular dielectric waveguides. Also, the attenuation is a slowly varying function of dimensions in the elliptical case, resulting in greater dimensional tolerances [6]–[9]. It follows that Goubau lines of elliptical cross sections should exhibit improved propagation characteristics over circular cases.

Karbowiak's [10] analysis of the elliptical Goubau line has very limited applications since he considered only one term in the infinite series for field expressions. Roumeliotis *et al.* [11] have obtained wavenumbers of certain modes in the above waveguide for small eccentricities only. Propagation characteristics of elliptical Goubau lines have not been reported.

In this work, the elliptical Goubau line is studied theoretically using the perturbation method and numerical results for propagation characteristics are presented.

II. FIELD COMPONENTS

The elliptical Goubau line consists of an elliptical cylindrical conductor coated with a confocal dielectric layer as shown in Fig. 1. Though a constant dielectric thickness

Manuscript received March 4, 1980; revised June 24, 1980. This paper was supported by the Natural Sciences and Engineering Research Council of Canada.

J. E. Lewis is with the Department of Electrical Engineering, University of New Brunswick, Fredericton, N.B. E3B 5A3 Canada.

S. R. Rengarajan was with the Department of Electrical Engineering, University of New Brunswick, Fredericton, N. B., E3B 5A3, Canada. He is now with the Electrical and Computer Engineering Department, California State University, Northridge, CA 91330.

0018-9480/80/1000-1089$00.75 ©1980 IEEE

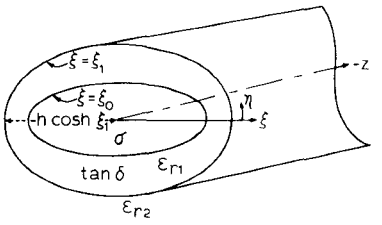

Fig. 1. Elliptical surface-wave transmission line and coordinate system.

would be of greater practical significance, the elliptical dielectric layer simplifies the analysis. Due to the lack of circular symmetry this waveguide can propagate only hybrid modes.

Omitting the $t-z$ dependence, $e^{j(\omega t-\beta z)}$, where β is the phase coefficient and ω is the angular frequency, the lossless axial fields in region i, $(i=1,2)$ for even modes are

$$E_{zi}=\sum_{m=1}^{\infty} a_m^{(i)}A_m^{(i)}(\xi,q_i)se_m(\eta,q_i)$$

$$H_{zi}=\sum_{m=0}^{\infty} b_m^{(i)}B_m^{(i)}(\xi,q_i)ce_m(\eta,q_i) \tag{1}$$

where $a_m^{(i)}$ and $b_m^{(i)}$ are arbitrary constants, and $A_m^{(i)}(\xi,q_i)$ and $B_m^{(i)}(\xi,q_i)$ are functions of modified Mathieu functions in region i. The functions for region 1 are chosen such that the tangential electric fields are zero on the conductor, while for region 2 all functions vanish at infinity.

The parameter q_i is given by

$$q_i=(k_i^2-\beta^2)h^2/4$$

where k_i is the wavenumber for region i and h is the semi-interfocal distance, and

$$A_m^{(1)}(\xi,q_1)=\begin{cases} Se_m(\xi,q_1)-\dfrac{Se_m(\xi_0,q_1)}{Gey_m(\xi_0,q_1)}Gey_m(\xi,q_1), & \text{for even modes} \\ Se_m(\xi,q_1)-\dfrac{Se_m'(\xi_0,q_1)}{Gey_m'(\xi_0,q_1)}Gey_m(\xi,q_1), & \text{for odd modes} \end{cases}$$

$$A_m^{(2)}(\xi,q_2)=Gek_m(\xi,q_2) \tag{2}$$

$$B_m^{(1)}(\xi,q_1)=\begin{cases} Ce_m(\xi,q_1)-\dfrac{Ce_m'(\xi_0,q_1)}{Fey_m'(\xi_0,q_1)}Fey_m(\xi,q_1), & \text{for even modes} \\ Ce_m(\xi,q_1)-\dfrac{Ce_m(\xi_0,q_1)}{Fey_m(\xi_0,q_1)}Fey_m(\xi,q_1), & \text{for odd modes} \end{cases}$$

$$B_m^{(2)}(\xi,q_2)=Fek_m(\xi,q_2). \tag{3}$$

Leaving the second term from (2) and (3) for $i=1$ yields the field expressions for the elliptical dielectric rod waveguide [6]. The transverse field components are

$$E_{\xi i}=-\frac{j}{(k_i^2-\beta^2)L}\left[\beta\sum_{m=1}^{\infty}a_m^{(i)}A_m^{(i)\prime}(\xi,q_i)se_m(\eta,q_i)+\omega\mu_i\sum_{m=0}^{\infty}b_m^{(i)}B_m^{(i)}(\xi,q_i)ce_m'(\eta,q_i)\right]$$

$$E_{\eta i}=-\frac{j}{(k_i^2-\beta^2)L}\left[\beta\sum_{m=1}^{\infty}a_m^{(i)}A_m^{(i)}(\xi,q_i)se_m'(\eta,q_i)-\omega\mu_i\sum_{m=0}^{\infty}b_m^{(i)}B_m^{(i)\prime}(\xi,q_i)ce_m(\eta,q_i)\right]$$

$$H_{\xi i}=-\frac{j}{(k_i^2-\beta^2)L}\left[-\omega\varepsilon_i\sum_{m=1}^{\infty}a_m^{(i)}A_m^{(i)}(\xi,q_i)se_m'(\eta,q_i)+\beta\sum_{m=0}^{\infty}b_m^{(i)}B_m^{(i)\prime}(\xi,q_i)ce_m(\eta,q_i)\right]$$

$$H_{\eta i}=-\frac{j}{(k_i^2-\beta^2)L}\left[\omega\varepsilon_i\sum_{m=1}^{\infty}a_m^{(i)}A_m^{(i)\prime}(\xi,q_i)se_m(\eta,q_i)+\beta\sum_{m=0}^{\infty}b_m^{(i)}B_m^{(i)}(\xi,q_i)ce_m'(\eta,q_i)\right] \tag{4}$$

where

$$L=h[(\cosh 2\xi-\cos 2\eta)/2]^{1/2}$$

and μ_i and ε_i are the permeability and permittivity of medium i, respectively. The field components for odd modes are obtained by the method given in Appendix A.

III. Characteristic Equations

The characteristic equations are obtained by matching the tangential fields at the boundary, $\xi=\xi_1$. Matching the axial fields given by (1) at $\xi=\xi_1$, and making use of orthogonality properties of Mathieu functions given in Appendix B, yields

$$a_r^{(1)}A_r^{(1)}(\xi_1,q_1)=\sum_{m=1}^{\infty'}a_m^{(2)}A_m^{(2)}(\xi_1,q_2)\beta_{m,r}$$

$$b_r^{(1)}B_r^{(1)}(\xi_1,q_1)=\sum_{m=0}^{\infty'}b_m^{(2)}B_m^{(2)}(\xi_1,q_2)\alpha_{m,r} \tag{5}$$

where $\alpha_{m,r}$ and $\beta_{m,r}$ are defined in Appendix B, and the prime over the summation sign means that either odd or even values of m are used, depending on whether r is odd or even.

Matching the azimuthal fields given by (4) at $\xi=\xi_1$ and making use of (5) to eliminate the arbitrary constants in region 1 and the use of orthogonality properties of Mathieu functions given in Appendix B yields two sets of infinite homogeneous equations

$$\sum_{m=1}^{\infty'}a_m^{(2)}e_{m,r}+\sum_{m=0}^{\infty'}b_m^{(2)}f_{m,r}=0$$

$$\sum_{m=1}^{\infty'}a_m^{(2)}g_{m,r}+\sum_{m=0}^{\infty'}b_m^{(2)}h_{m,r}=0 \tag{6}$$

where the functions e, f, g, h are defined in Appendix C.

In order that (6) may be satisfied, the infinite determinant of the system must be set to zero. This determinental equation, which is the characteristic equation takes two forms depending on m and r being odd or even. For odd values of m and r

$$\begin{vmatrix} e_{11} & f_{11} & e_{31} & f_{31} & \cdot & \cdot \\ g_{11} & h_{11} & g_{31} & h_{31} & \cdot & \cdot \\ e_{13} & f_{13} & e_{33} & f_{33} & \cdot & \cdot \\ g_{13} & h_{13} & g_{33} & h_{33} & \cdot & \cdot \\ \cdot & \cdot & \cdot & \cdot & \cdot & \cdot \\ \cdot & \cdot & \cdot & \cdot & \cdot & \cdot \end{vmatrix} = 0. \tag{7}$$

While for even values of m and r

$$\begin{vmatrix} h_{00} & g_{20} & h_{20} & g_{40} & h_{40} & \cdot & \cdot \\ f_{02} & e_{22} & f_{22} & e_{42} & f_{42} & \cdot & \cdot \\ h_{02} & g_{22} & h_{22} & g_{42} & h_{42} & \cdot & \cdot \\ f_{04} & e_{24} & f_{24} & e_{44} & f_{44} & \cdot & \cdot \\ h_{04} & g_{24} & h_{24} & g_{44} & h_{44} & \cdot & \cdot \\ \cdot & \cdot & \cdot & \cdot & \cdot & \cdot & \cdot \\ \cdot & \cdot & \cdot & \cdot & \cdot & \cdot & \cdot \end{vmatrix} = 0. \tag{8}$$

The characteristic equations for odd modes can be obtained from (6) using the method given in Appendix A. They may also be obtained from (7) and (8) by interchanging ε's and μ's and changing the signs of $f_{m,r}$ and $g_{m,r}$ for all m and r. Characteristic equations similar to (7) and (8) have been obtained for elliptical dielectric waveguides [6], [12].

IV. Mode Spectra

The mode spectra for odd and even hybrid modes are obtained by a numerical solution of the characteristic equations and are shown in Fig. 2. The required Mathieu functions and related parameters are generated by an accurate algorithm [13]. The mode designation is obtained from the sequence of solutions and by comparing the modes for the circular and elliptical cross sections. The ${}_eHE_{mn}({}_eEH_{mn})$ and ${}_oHE_{mn}({}_oEH_{mn})$ modes degenerate to the well known $HE_{mn}(EH_{mn})$ modes of the circular Goubau line as the elliptical cross section degenerates to the circular case, while ${}_eHE_{0n}({}_oEH_{0n})$ modes become $H_{0n}(E_{0n})$ modes. It is observed from Fig. 2 that the ${}_oEH_{01}$, ${}_eHE_{11}$, and ${}_oHE_{11}$ modes have zero cutoff frequencies, as do the corresponding E_{01} and HE_{11} modes in the circularly symmetric case [2].

It has been reported [6]–[8] that the infinite determinantal equations in the case of elliptical dielectric waveguides are fast convergent for other than high eccentricities. This behavior also has been observed for the case under study.

A. Field Distribution

The arbitrary constants in region 2 at any point on a given mode are obtained by the singular value decomposition method [14]. The constants in region 1 are obtained from (5) and the field components can then be computed from (1) and (4). It has been found that even though the characteristic equations are fast convergent, the size of the characteristic determinant is required to be relatively large to produce good field matching at the boundary. In this work, characteristic determinants up to order 12 were used, depending on eccentricity, phase constant, and normalized wavelength.

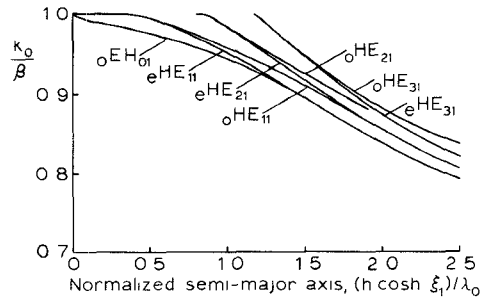

Fig. 2. Mode spectrum of the elliptical surface-wave transmission line for $\varepsilon_{r1}=2.26$, $\varepsilon_{r2}=1.0$, $\xi_0=0.909$, $\xi_1=1.0$.

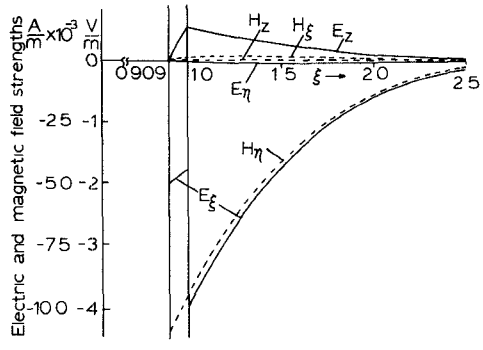

Fig. 3. Radial dependence of electric and magnetic fields of the ${}_oEH_{01}$ mode for $\varepsilon_{r1}=2.26$, $\varepsilon_{r2}=1.0$, $k_0/\beta=0.974$, $(h\cosh\xi_1)/\lambda_0=0.524$.

Typical plots of the radial variation of the electric and magnetic field components for ${}_oEH_{01}$ mode are shown in Fig. 3. The ${}_eHE_{11}$ and ${}_oHE_{11}$ modes are found to have similar characteristics. However the angular variation of $HE_{mn}(EH_{mn})$ modes have primarily a harmonic variation of order m.

V. Propagation Characteristics

A. Phase Characteristics

The phase characteristics are obtained by numerical solution of the characteristic equations. The phase characteristics of ${}_oEH_{01}$, ${}_eHE_{11}$, and ${}_oHE_{11}$ modes for different dielectric constants, dielectric thicknesses, and eccentricities are illustrated in Fig. 4(a), (b), and (c). It is found that, even though it has zero cutoff frequency, the ${}_oHE_{11}$ mode has the highest value of normalized phase velocity at any given frequency and hence it is the weakest guided mode. Near cutoff, the phase characteristics of the ${}_eHE_{11}$ mode resemble those of ${}_oHE_{11}$ mode, whereas far-above cutoff the phase velocity approaches that of the ${}_oEH_{01}$ mode. From Fig. 2 it is found that higher order

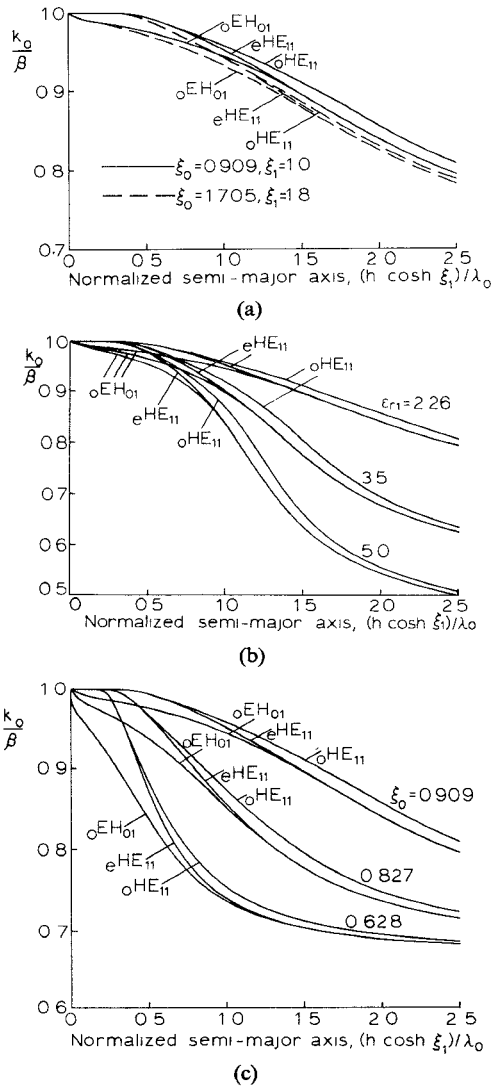

Fig. 4. (a) Phase characteristics for different eccentricities, $\varepsilon_{r1}=2.26$, $\varepsilon_{r2}=1.0$. (b) Phase characteristics for different dielectric constants, $\xi_0=0.909$, $\xi_1=1.0$, $\varepsilon_{r2}=1.0$. (c) Phase characteristics for different dielectric thicknesses for $\varepsilon_{r1}=2.26$, $\varepsilon_{r2}=1.0$, $\xi_1=1.0$.

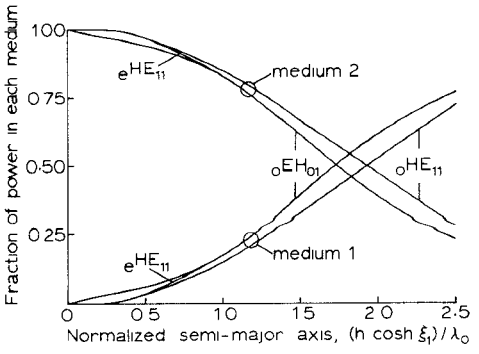

Fig. 5. Power distribution characteristics for $\varepsilon_{r1}=2.26$, $\varepsilon_{r2}=1.0$, $\xi_0=0.909$, $\xi_1=1.0$.

modes have more rapid variation of their characteristics with dimensions, particularly near cutoff.

The normalized phase velocity increases with eccentricity and decreases with increasing dielectric constant or thickness. The separation between the phase plots of ${}_oEH_{01}$ and ${}_oHE_{11}$ modes increases with eccentricity.

B. Power Flow

The power flow though medium i is given by

$$F_i=\frac{1}{2}\int_{\xi_{i-1}}^{\xi_i}\int_0^{2\pi}(E_{\xi i}H_{\eta i}^*-E_{\eta i}H_{\xi i}^*)L^2\,d\eta\,d\xi \tag{9}$$

where $\xi_2=\infty$. Substituting the expressions for E_ξ, H_η, E_η, and H_ξ from (4) in (9) yields for even modes

$$\begin{aligned}2F_i=\frac{\beta\omega\mu_i}{h_i^4}\int_{\xi_{i-1}}^{\xi_i}\Bigg[&\sum_{m=0}^{\infty'} b_m^{(i)2}\{\pi B_m^{(i)'2}(\xi,q_i)\\&+C_{m,m}^{(i)}B_m^{(i)2}(\xi,q_i)\}+\sum_{m=1}^{\infty'}a_m^{(i)2}\frac{\varepsilon_i}{\mu_i}\\&\cdot\{\pi A_m^{(i)'2}(\xi,q_i)+S_{m,m}^{(i)}A_m^{(i)2}(\xi,q_i)\}\Bigg]d\xi\\&+\frac{(\beta^2+\omega^2\mu_i\varepsilon_i)}{h_i^4}\sum_{m=0}^{\infty'}\sum_{n=1}^{\infty'}b_m^{(i)}a_n^{(i)}T_{m,n}^{(i)}\\&\cdot\left[B_m^{(i)}(\xi,q_i)A_n^{(i)}(\xi,q_i)\right]_{\xi_{i-1}}^{\xi_i}\\&+\frac{2\beta\omega\mu_i}{h_i^4}\sum_{m=0}^{\infty'}\sum_{n=m+2}^{\infty'}b_m^{(i)}b_n^{(i)}C_{m,n}^{(i)}\\&\cdot\left[B_m^{(i)'}(\xi,q_i)B_n^{(i)}(\xi,q_i)-B_m^{(i)}(\xi,q_i)B_n^{(i)'}(\xi,q_i)\right]_{\xi_{i-1}}^{\xi_i}\\&\cdot\left[a_m(q_i)-a_n(q_i)\right]^{-1}+\frac{2\beta\omega\varepsilon_i}{h_i^4}\sum_{m=1}^{\infty'}\sum_{n=m+2}^{\infty'}a_m^{(i)}a_n^{(i)}S_{m,n}^{(i)}\\&\cdot\left[A_m^{(i)'}(\xi,q_i)A_n^{(i)}(\xi,q_i)-A_m^{(i)}(\xi,q_i)A_n^{(i)'}(\xi,q_i)\right]_{\xi_{i-1}}^{\xi_i}\\&\cdot\left[b_m(q_i)-b_n(q_i)\right]^{-1}\end{aligned} \tag{10}$$

where $a_m(q_i)$ and $b_m(q_i)$ are the characteristic values of even and odd Mathieu functions of order m, respectively. The angular integrals $C_{m,n}^{(i)}$, $S_{m,n}^{(i)}$, and $T_{m,n}^{(i)}$ are defined in Appendix D and the primes over the summation indicate that only odd or even integral values are used.

The power flow expression for odd modes is obtained by the method given in Appendix A.

The fractional power carried by media 1 and 2 for ${}_oEH_{01}$, ${}_eHE_{11}$, and ${}_oHE_{11}$ modes is shown in Fig. 5. Most of the power is carried in medium 2 near cutoff and in medium 1 far above cutoff. Among these three modes at any given normalized frequency the ${}_oHE_{11}$ mode carries the largest fraction of power in medium 2.

Since the Goubau line is an open structure it is subject to radiation and interference at bends or discontinuities. It may be shielded by being embedded in a material such as polyfoam as suggested for the dielectric tube waveguide [15]. The power concentration characteristics of Goubau lines are illustrated in Fig. 6 which shows a plot of the semi-major axis of the ellipse within which 99.9 percent of

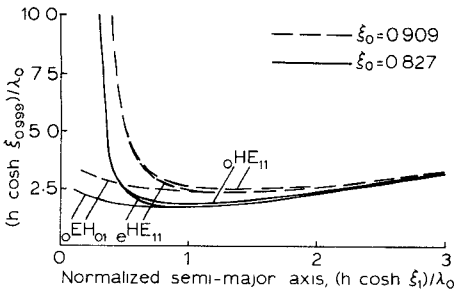

Fig. 6. Power concentration characteristics for different dielectric thicknesses, $\varepsilon_{r1}=2.26$, $\varepsilon_{r2}=1.0$, $\xi_1=1.0$.

the total power is contained versus the semimajor axis of the outer boundary ellipse, both normalized to free-space wavelength. It is seen that power concentration near the guide decreases with eccentricity. It is seen also from Fig. 6 that the ${}_oHE_{11}$ mode has the largest radial extension of the three modes considered.

C. Energy Storage

The energy stored per unit length in medium i is given by

$$W_i=\frac{\varepsilon_i}{2}\int_{\xi_{i-1}}^{\xi_i}\int_0^{2\pi}\left[|E_{zi}|^2+|E_{\xi i}|^2+|E_{\eta i}|^2\right]L^2\,d\eta\,d\xi \quad (11)$$

where $\xi_2=\infty$. Using (1) and (4) in (11) yields for the even modes

$$\begin{aligned}\frac{2}{\varepsilon_i}W_i=&\int_{\xi_{i-1}}^{\xi_i}\Bigg[\sum_{m=0}^{\infty'}b_m^{(i)^2}\frac{\omega^2\mu_i}{h_i^4}\left\{\pi B_m^{(i)'^2}(\xi,q_i)+C_{m,m}^{(i)}B_m^{(i)^2}(\xi,q_i)\right\}\\&+\sum_{m=1}^{\infty'}a_m^{(i)^2}\frac{\beta^2\pi}{h_i^4}A_m^{(i)'^2}(\xi,q_i)+\sum_{m=1}^{\infty'}A_m^{(i)^2}(\xi,q_i)\\&\cdot\left\{-\frac{h^2}{2}V_{m,m}^{(i)}+\frac{\beta^2}{h_i^4}S_{m,m}^{(i)}+\frac{h^2}{2}\pi\cosh 2\xi\right\}a_m^{(i)^2}\Bigg]d\xi\\&+\sum_{m=1}^{\infty'}\sum_{n=m+2}^{\infty'}\left\{-h^2V_{m,n}^{(i)}+\frac{2\beta^2}{h_i^4}S_{m,n}^{(i)}\right\}a_m^{(i)}a_n^{(i)}\\&\cdot\left[A_m^{(i)'}(\xi,q_i)A_n^{(i)}(\xi,q_i)-A_m^{(i)}(\xi,q_i)A_n^{(i)'}(\xi,q_i)\right]_{\xi_{i-1}}^{\xi_i}\\&\cdot\left[b_m(q_i)-b_n(q_i)\right]^{-1}+\frac{2\omega^2\mu_i^2}{h_i^4}\sum_{m=0}^{\infty'}\sum_{n=m+2}^{\infty'}b_m^{(i)}b_n^{(i)}C_{m,n}^{(i)}\\&\cdot\left[B_m^{(i)'}(\xi,q_i)B_n^{(i)}(\xi,q_i)-B_m^{(i)}(\xi,q_i)B_n^{(i)'}(\xi,q_i)\right]_{\xi_{i-1}}^{\xi_i}\\&\cdot\left[a_m(q_i)-a_n(q_i)\right]^{-1}+\frac{2\omega\mu_i\beta}{h_i^4}\sum_{m=0}^{\infty'}\sum_{n=1}^{\infty'}b_m^{(i)}a_n^{(i)}T_{m,n}^{(i)}\\&\cdot\left[B_m^{(i)}(\xi,q_i)A_n^{(i)}(\xi,q_i)\right]_{\xi_{i-1}}^{\xi_i}\end{aligned} \quad (12)$$

where the integrals $C_{m,n}^{(i)}$, $S_{m,n}^{(i)}$, $T_{m,n}^{(i)}$, and $V_{m,n}^{(i)}$ are defined in Appendix D. The expression for odd modes is obtained from (12) by the method in Appendix A.

D. Power Loss

Power loss per unit length N_i in a dielectric is obtained by the perturbation method.

$$N_i=\omega\tan\delta_i\,W_i \quad (13)$$

where $\tan\delta_i$ is the loss and W_i is the energy stored in the medium.

The power loss tangent in the conductor is obtained by a perturbation method from the lossless fields. The conventional perturbation method to find the power loss in a hollow conducting waveguide using the intrinsic impedance of the metal as the surface impedance has been shown to be applicable to elliptical cross section [16]. The conductor power loss per unit length for the Goubau line is given by

$$P_c=\frac{1}{2}\int_0^{2\pi}|H_{z1}|^2R_mL\,d\eta+\frac{1}{2}\int_0^{2\pi}|H_{\eta 1}|^2R_mL\,d\eta \quad (14)$$

where $R_m=\sqrt{\frac{\omega\mu}{2\sigma}}$, μ is the permeability, and σ is the conductivity of the metal. Substituting for H_{z1} and $H_{\eta 1}$ from (1) and (4) in (14) yields for even modes

$$\begin{aligned}P_c=&\frac{R_m}{2}h\cosh\xi_0\Bigg[\sum_{m=0}^{\infty'}\sum_{n=0}^{\infty'}b_m^{(1)}b_n^{(1)}B_m^{(1)}(\xi_0,q_1)B_n^{(1)}(\xi_0,q_1)\\&\cdot\int_0^{2\pi}ce_m(\eta,q_1)ce_n(\eta,q_1)\sqrt{1-e^2\cos^2\eta}\,d\eta\Bigg]\\&+\frac{R_m}{2h_1^4h\cosh\xi_0}\Bigg[\beta^2\sum_{m=0}^{\infty'}\sum_{n=0}^{\infty'}b_m^{(1)}b_n^{(1)}B_m^{(1)}(\xi_0,q_1)\\&\cdot B_n^{(1)}(\xi_0,q_1)\int_0^{2\pi}\frac{ce_m'(\eta,q_1)ce_n'(\eta,q_1)}{\sqrt{1-e^2\cos^2\eta}}\,d\eta\\&+\omega^2\varepsilon_1^2\sum_{m=1}^{\infty'}\sum_{n=1}^{\infty'}a_m^{(1)}a_n^{(1)}A_m^{(1)'}(\xi_0,q_1)A_n^{(1)'}(\xi_0,q_1)\\&\cdot\int_0^{2\pi}\frac{se_m(\eta,q_1)se_n(\eta,q_1)}{\sqrt{1-e^2\cos^2\eta}}d\eta\\&+2\omega\varepsilon_1\beta\sum_{m=0}^{\infty'}\sum_{n=1}^{\infty'}b_m^{(1)}a_n^{(1)}B_m^{(1)}(\xi_0,q_1)A_n^{(1)'}(\xi_0,q_1)\\&\cdot\int_0^{2\pi}\frac{ce_m'(\eta,q_1)se_n(\eta,q_1)}{\sqrt{1-e^2\cos^2\eta}}d\eta\Bigg]\end{aligned} \quad (15)$$

where $e=1/\cosh\xi_0$ is the eccentricity of the elliptical cross section of the conductor boundary. A similar result for odd modes may be obtained from (15) by the method described in Appendix A.

E. Attenuation Characteristics

The attenuation coefficient is obtained from computed values of power loss and power flow. The attenuation characteristics of three low-order modes are shown in Fig. 7 for different dielectric thicknesses and eccentricities.

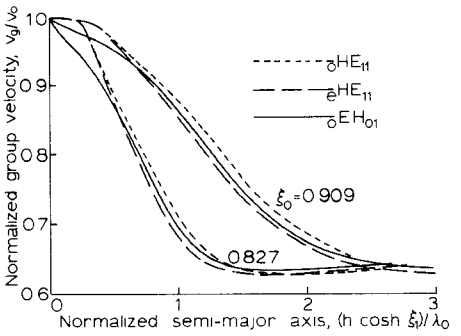

Fig. 7. Attentuation characteristics, $\varepsilon_{r1}=2.26$, $\varepsilon_{r2}=1.0$, $\tan\delta=5\cdot10^{-4}$, $\sigma=5.8\cdot10^7$ S/m, $h\cosh\xi_1=1.0$ cm.

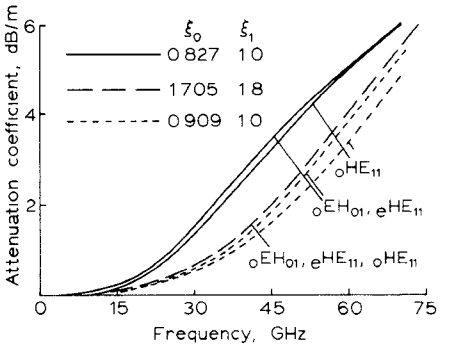

Fig. 8. Group velocity characteristics for different dielectric thicknesses, $\varepsilon_{r1}=2.26$, $\varepsilon_{r2}=1.0$, $\xi_1=1.0$.

The attenuation increases with dielectric thickness. As predicted by phase and power flow characteristics, $_oHE_{11}$ mode has the lowest attenuation at any given normalized frequency. Also the attenuation is a very slowly-varying function of dimensions in lines of high eccentricities. The difference in attenuation between the $_oHE_{11}$ and $_oEH_{01}$ modes increases with eccentricity.

G. Group Velocity

The group velocity can be obtained from the power flow and energy storage per unit length

$$v_g = \sum_{i=1}^{2} F_i / \sum_{i=1}^{2} W_i \tag{16}$$

where F_i and W_i can be computed from (10) and (12). Group velocity characteristics normalized to the free space velocity v_0 of a line for two dielectric thicknesses are shown in Fig. 8. Near cutoff group velocity is close to the free space value, while far above cutoff, it approaches the velocity of TEM waves in the dielectric.

VI. Conclusion

In this work, results of a comprehensive study of the propagation characteristics of elliptical surface wave transmission lines are presented. The mode spectrum shows a direct correspondence to that of the circularly symmetric case. Two orthogonally polarized degenerate HE_{11} modes in the circular waveguide are split into non-degenerate even and odd HE_{11} modes in the elliptical case. Propagation characteristics of nearly degenerate E_{01} and HE_{11} modes in the circular case are widely separated in the $_oEH_{01}$ and HE_{11} modes of the elliptical guide. The $_oEH_{01}$ and HE_{11} modes in the elliptical waveguide have lower attenuation than the corresponding modes in the circular case. Also, the propagation characteristics of Goubau lines of high eccentricities are slowly varying functions of transverse dimensions and frequency. Hence the elliptical waveguides have the advantage of greater dimensional tolerances over the circular ones. The $_oHE_{11}$ mode in the elliptical line is weakly bound to the line and has possible application in low loss transmission particularly in millimeter wave frequencies.

Appendix A

Functions to be interchanged to obtain expressions for odd modes from those of even modes

$a_m^{(i)}$	$b_m^{(i)}$
$A_m^{(i)}(\xi, q_i)$	$B_m^{(i)}(\xi, q_i)$
$A_m^{(i)'}(\xi, q_i)$	$B_m^{(i)'}(\xi, q_i)$
$se_m(\eta, q_i)$	$ce_m(\eta, q_i)$
$se'_m(\eta, q_i)$	$ce'_m(\eta, q_i)$
$S_{m,n}^{(i)}$	$C_{m,n}^{(i)}$
$V_{m,n}^{(i)}$	$U_{m,n}^{(i)}$

$T_{m,n}^{(i)}$	$-T_{m,n}^{(i)}$
$b_m(q_i)$	$a_m(q_i)$
$\alpha_{m,r}$	$\beta_{m,r}$
$\psi_{m,r}$	$\nu_{m,r}$.

Appendix B

Relations between Mathieu functions and derivatives in different regions

$$\alpha_{r,n}=\frac{\int_0^{2\pi} ce_r(\eta,q_2)ce_n(\eta,q_1)\,d\eta}{\int_0^{2\pi} ce_n^2(\eta,q_1)\,d\eta}$$

$$\beta_{r,n}=\frac{\int_0^{2\pi} se_r(\eta,q_2)se_n(\eta,q_1)\,d\eta}{\int_0^{2\pi} se_n^2(\eta,q_1)\,d\eta}$$

$$\psi_{r,n}=\frac{\int_0^{2\pi} ce_r'(\eta,q_1)se_n(\eta,q_1)\,d\eta}{\int_0^{2\Pi} se_n^2(\eta,q_1)\,d\eta}$$

$$\nu_{r,n}=\frac{\int_0^{2\pi} se_r'(\eta,q_1)ce_n(\eta,q_1)\,d\eta}{\int_0^{2\pi} ce_n^2(\eta,q_1)\,d\eta}.$$

Appendix C

Elements in the characteristic determinant

$$e_{m,r}=\frac{\omega\beta_{m,r}}{\beta}\left[\varepsilon_1\frac{A_r^{(1)'}(\xi_1,q_1)}{A_r^{(1)}(\xi_1,q_1)}A_m^{(2)}(\xi_1,q_2)-\frac{h_1^2}{h_2^2}\varepsilon_2 A_m^{(2)'}(\xi_1,q_2)\right]$$

$$f_{m,r}=\left(1-\frac{h_1^2}{h_2^2}\right)B_m^{(2)}(\xi_1,q_2)\sum_{n=0}^{\infty'}\alpha_{m,n}\psi_{n,r}$$

$$g_{m,r}=-\left(1-\frac{h_1^2}{h_2^2}\right)A_m^{(2)}(\xi_1,q_2)\sum_{n=1}^{\infty'}\beta_{m,n}\nu_{n,r}$$

$$h_{m,r}=\frac{\omega\alpha_{m,r}}{\beta}\left[\mu_1 B_m^{(2)}(\xi_1,q_2)\frac{B_r^{(1)'}(\xi_1,q_1)}{B_r^{(1)}(\xi_1,q_1)}-\frac{h_1^2}{h_2^2}\mu_2 B_m^{(2)'}(\xi_1,q_2)\right].$$

Appendix D

Integrals involving products of angular Mathieu functions and derivatives in Sections V-B and V-C

$$V_{m,n}^{(i)}=\int_0^{2\pi} se_m(\eta,q_i)se_n(\eta,q_i)\cos 2\eta\,d\eta$$

$$U_{m,n}^{(i)}=\int_0^{2\pi} ce_m(\eta,q_i)ce_n(\eta,q_i)\cos 2\eta\,d\eta$$

$$C_{m,n}^{(i)}=\int_0^{2\pi} ce_m'(\eta,q_i)ce_n'(\eta,q_i)\,d\eta$$

$$S_{m,n}^{(i)}=\int_0^{2\pi} se_m'(\eta,q_i)se_n'(\eta,q_i)\,d\eta$$

$$T_{m,n}^{(i)}=\int_0^{2\pi} ce_m'(\eta,q_i)se_n(\eta,q_i)\,d\eta.$$

References

[1] G. Goubau, "Surface waves and their application to transmission lines," *J. Appl. Phys.*, vol. 21, pp. 1119–1128, Nov. 1950.

[2] N. A. Semenov, "Wave modes in a surface-wave line," *Radio Eng. Electron. Phys.*, vol. 9, pp. 989–995, Sept. 1964.

[3] ——, "Parameters of an *E* wave in a surface wave line," *Radio Eng. Electron. Phys.*, vol. 9, pp. 1349–1355, July 1964.

[4] M. J. King and J. C. Wiltse, "Surface-wave propagation on coated or uncoated metal wires at millimeter wavelengths," *IRE Trans. Antennas Propagat.*, vol. AP-10, pp. 246–254, May 1962.

[5] J. G. Fikioris and J. A. Roumeliotis, "Cut-off wave numbers of Goubau lines, *IEEE Trans. Microwave Theory Tech.*, vol. MTT-27, pp. 570–573, June 1979.

[6] C. Yeh, "Elliptical dielectric waveguides," *J. Appl. Phys.*, vol. 33, pp. 3235–3243, Nov. 1962.

[7] ——, "Attenuation in a dielectric elliptical cylinder," *IEEE Trans. Antennas Propagat.*, vol. AP-11, pp. 177–184, Mar. 1963.

[8] J. E. Lewis and G. Deshpande, "Modes on elliptical cross-section dielectric-tube waveguides," *IEE J. Microwaves, Optics, Acoust.*, vol. 3, pp. 147–155, July 1979.

[9] S. R. Rengarajan and J. E. Lewis, "Propagation characteristics of elliptical dielectric-tube waveguides," *Proc. IEE*, vol. 127, Part H, Microwaves, Optics and Antennas, June 1980.

[10] A. E. Karbowiak, "The elliptic surface wave," *Brit. J. Appl. Phys.*, vol. 5, pp. 328–335, Sept. 1954.

[11] J. A. Roumeliotis, A. B. M. Siddique Houssain, and J. G. Fikioris, "Metallic and Goubau waveguides with eccentric circular and concentric circular-elliptic cross section," in *Proc. 8th European Microwave Conf.*, (Paris, France), pp. 446–450, Sept. 1978.

[12] S. R. Rengarajan and J. E. Lewis, "First higher-mode cutoff in two-layer elliptical fibre waveguides," *Electron. Lett.*, vol. 16, pp. 263–264, Mar. 1980.

[13] ——, "Mathieu functions of integral orders and real arguments," *IEEE Trans. Microwave Theory Tech.*, vol. MTT-28, pp. 276–277, Mar. 1980.

[14] G. H. Golub and C. Reinsch, "Singular value decomposition and least squares solutions," *Numer. Math.*, vol. 14, pp. 403–420, 1970.

[15] M. M. Z. Kharadly and J. E. Lewis, "Properties of dielectric tube waveguides," *Proc. IEE*, vol. 116, pp. 214–224, 1969.

[16] S. R. Rengarajan and J. E. Lewis, "Surface impedance of elliptical hollow conducting waveguides," *Electron. Lett.*, vol. 15, pp. 637–639, Oct. 1979.